Law of Sines Based Approach for the Accurate Orientation Determination

Merve Kaya[1], Nezir Doğan[2], Önder Halis Bettemir[3]

[1]İnönü University, Engineering Faculty, 44280 Malatya, Türkiye - kya.mrw@gmail.com
[2]İnönü University, Engineering Faculty, 44280 Malatya, Türkiye - nezirdogan22@gmail.com
[3]İnönü University, Engineering Faculty, 44280 Malatya, Türkiye - onder.bettemir@inonu.edu.tr

Keywords: Law of Sines, Orientation, Digital Twin, Autonomous Navigation.

Abstract

Thanks to developing sensor technologies and autonomous systems, modelling buildings with environmental data and the digital twin approach are becoming increasingly important. This study examines the environmental perception, obstacle detection, and directional correction capabilities of an autonomous vehicle equipped with on board distance sensors integrated with building information modelling (BIM). The vehicle operating around a building detects obstacles through its on board sensors while maintaining its motion parallel to the building wall. Possible angle and direction deviations during movement are determined using the geometry of a triangle formed by three distance measurements taken from specific angles with ultrasonic sensors and the sine theorem. The resulting environmental map from the obtained data will form the basis for digital twin modelling. Instead of using expensive sensors to determine direction, this study uses a method that determines the vehicle's direction using geometry based on the sine theorem and three distance measurements taken from different angles. Field studies have not encountered any adverse events other than erroneous distance measurements due to sensor echo detection. The direction determination method developed in this study is expected to be particularly beneficial for mapping and creating digital twins of buildings.

1. Introduction

Digitalization is defined as the process of integrating digital technologies into business models, processes, and organizational structures, leading to radical changes and impacting the socio-technical aspects of construction (Yoo et al., 2010; Fichman et al., 2014). The construction industry faces fundamental problems such as low productivity, high costs, sustainability, and the inability to achieve the desired quality. Recently, digitalization has brought about a rapid transformation in the construction sector, as in many other sectors. The adoption of technologies developed through digitalization in the construction sector is considered a potential solution to these problems. A large amount of data is generated throughout the lifecycle of a construction project, and project success depends on the insights derived from the effective management and analysis of this data. Research emphasizes the importance of information management as an integral part of construction projects and the processes through which information is generated, communicated, and interpreted. However, the literature has largely focused on the design and construction phases, which account for only 30-40% of the total project cost. The true cost, which accounts for 60-80% of the total cost, arises during the operation and usage phase (El jazzar, 2020). Especially in large-scale projects, developing data-driven decision-making processes provides significant advantages in terms of both cost and time. In this context, digital twin technology, which has recently gained popularity, is considered a concept that offers innovative solutions to existing problems and transforms physical data into usable data for decision-making. Data integration involves transferring data from the physical world to the virtual model and vice versa, allowing simulations to be used to improve real-world operations (Qi and Tao, 2018). However, one of the most crucial stages in creating digital twins is the data collection phase, and obtaining highly accurate and reliable data is necessary to create twins that consistently reflect the true model. The data collection process is significantly challenging due to uncertainties in field conditions, limited accuracy of measurement devices, and errors resulting from human factors. Therefore, new methods are needed to both increase efficiency and enhance measurement reliability. Autonomous and sensor-based approaches are at the forefront in this regard.

This study aims to obtain distance data and analyse the impact of angular deviations on measurement accuracy by integrating ultrasonic sensors into a vehicle that can move autonomously around a building. The autonomous vehicle's mobility allows the sensors to perform measurements at different orientation angles, thus minimizing human intervention.

The developed system uses distance measurement data obtained from sensors to calculate angle deviations and interprets them as the side lengths of the triangle formed by the sensors. The vehicle's deviation angle is calculated by applying the sine theorem to the resulting triangle geometry. This method uses distance sensor data and the angles between the sensors to calculate the vehicle's deviation angle.

The study aims to simplify the data collection phase, which is fundamental to creating a digital twin. Furthermore, ultrasonic distance sensors were used to ensure cost-effectiveness. With the vehicle's autonomy, human intervention will be minimized. The sensors used and the algorithm to be developed will provide the vehicle with decision-making capabilities, helping to complete the mapping and obstacle detection processes with high accuracy and in a shorter time.

2. Literature Review

Design and management tools used in construction projects have evolved over time, from paper drawings to CAD, Building Information Modelling (BIM), and Geographic Information Systems (GIS) (Hasan et al. 2022). In recent years, BIM has made significant strides in information management. BIM has transformed the construction industry from 2D-based systems to 3D-object-based systems, making the information needed throughout the project lifecycle more accessible. However, BIM

cannot fully capture the data generated during the operation and usage phases. Digital Twin technology, a key element of Industry 4.0, is emerging to address this shortcoming.

The origins of the digital twin concept are first seen in the aviation and space field. The foundations of this approach date back to NASA's Apollo project in the 1960s (Shafto et al., 2010; Negri et al., 2017; Boschert et al., 2018). However, the "twin" referred to at that time was a purely physical system (Zhuang et al., 2018). The digital dimension had not yet been incorporated into the concept at that time. The term "digital twin" was first coined by Grievens in 2003 during a course he gave on product lifecycle management (PLM) (Grieves, 2014). The definition of a digital twin has evolved over time, focusing on three main components: the physical object, the virtual representation, and the data that connects these two spaces. The data collection phase of creating a digital twin is crucial for its accuracy. Furthermore, data collection methods are costly, labor-intensive, and time-consuming. Therefore, the development of low-cost autonomous vehicle systems capable of environmental scanning both automates the data collection process in digital twin production and minimizes human intervention. Wall-tracking algorithms, especially maze-solving algorithms, are widely used for autonomous vehicle movement.

Suthar and Shukla (2023) developed a robot powered by infrared sensors and a left-hand-wall-following algorithm to determine its orientation, demonstrating a 70% success rate in completing a maze.

Similarly, Suryanarayana et al. (2021) demonstrated that a robot they developed using ultrasonic sensors successfully completed a maze using a left-handed algorithm and acting in harmony with environmental factors. In their study, the robot made directional decisions based on sensor data and was able to detect intersection types.

Khaleel and Oleiwi (2024) developed a decision-making algorithm that allows autonomous mobile robots to navigate a maze without hitting the walls. Ultrasonic sensors were used to avoid obstacles, allowing the robot to move flexibly according to measured distances. The robot scans its environment from 0 to 180 degrees to determine its orientation and can reach the target by avoiding obstacles in 60 seconds. It has been seen that low-cost applications can also yield effective results by using Arduino Uno and L298N motor driver as hardware.

Pandian et al. (2012) developed an algorithm they called LSRB (Left-Straight-Right-Back). Using this algorithm, a maze-solving robot was developed, enabling the robot to find the shortest path by optimizing its decision sequences. Such algorithms enable vehicles navigating autonomously around buildings to detect building geometry and perform both position correction and environmental mapping.

3. Method

This study aimed to develop a vehicle that can autonomously detect and model the building's surroundings and any obstacles within them. The environment in which the vehicle will operate and the obstacles it may encounter are shown in Figure 1.

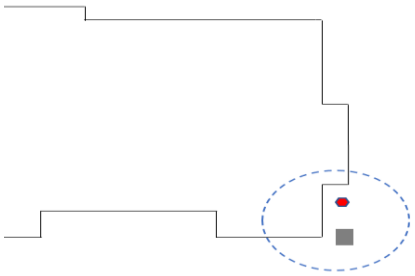

Figure 1. Illustration of a typical obstacle during the mapping of a building facade.

The vehicle may experience some directional and angular deviations due to environmental or mechanical factors while the vehicle is in motion. This is illustrated in Figure 2.

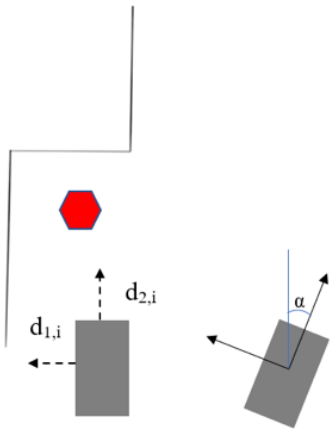

Figure 2. Illustration of deviation of the heading angle.

In Figure 2, (x_i, y_i) represents the vehicle's location coordinates at time i, (X_i , Y_i) represents the building's location at time i, $d_{1,i}$ and $d_{2,i}$ represent the distance data at time i obtained from the ultrasonic sensors installed, and angle α represents the angle the vehicle makes with respect to the north. As the vehicle continues to move, its location information will be updated. For each advancement time of Δt, the vehicle's location will be calculated as shown in Equation 1. The vehicle will be considered to be moving at a constant speed *V*.

$$x_{i+1} = x_i + V_i * \Delta t \;\; ; \;\; y_{i+1} = y_i + V_i * \Delta t \qquad (1)$$

These equations will provide a high degree of accuracy when used under conditions where the vehicle is moving at a specific speed and in a constant direction. However, the vehicle will not always move in the same direction; even a small bump in front of it can cause a deviation in the direction of movement. In this case, the calculations will be made as in Equation 2, taking into account the direction angle.

$$x_{i+1} = x_i + V_i * \Delta t * \sin\alpha_i \;\; ; \;\; y_{i+1} = y_i + V_i * \Delta t * \cos\alpha_i \qquad (2)$$

The direction angle α, which will be used in calculating vehicle and building positions, will be determined using distance readings from ultrasonic sensors and the sine theorem. The situation that will occur if the vehicle deviates is shown in Figure 3.

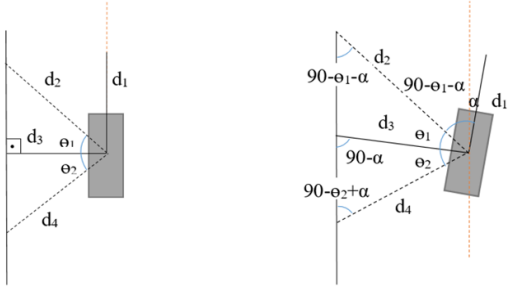

Figure 3. Representation of the measurement of the heading angle by law of sines.

Equation 3 will be used to find the angle that the vehicle makes with the north direction.

$$\frac{d_2}{\sin(90-\theta_2+\alpha)} = \frac{d_4}{\sin(90-\theta_1-\alpha)} \quad (3)$$

The vehicle is equipped with sensors that measure distances at specific angles. Values obtained from various sensors are used in the calculation. Here, the distances d_2 and d_4 are measured by ultrasonic sensors and are known data. The angle $ɵ_1$ and $ɵ_2$ is the angle between the installed sensors and is also known. When the equation is solved, the direction angle of the vehicle at moment i is obtained.

The vehicle position for time i is determined using the resulting angle α value in equation 2. The building position is determined based on the vehicle position. After the vehicle advances for a time period of t, it reaches time i+1, and the building position is calculated according to Equation 4.

$$X_{i+1} = x_{i+1} \pm * d_{1,i+1} * \sin\alpha_{i+1};\ Y_{i+1} = y_{i+1} \pm * d_{1,i+1} * \cos\alpha_{i+1} \quad (4)$$

To determine the angle α to be used in calculating the target surface's position, three different geometric models were created based on the sine theorem. First, a large triangle model was used, encompassing the distance values d_2 and d_4 and the angle values θ_1 and θ_2, to obtain the angle α. Subsequently, to increase measurement precision and obtain more consistent results across different situations, two smaller triangle models were also created separately within the large triangle. The side-angle relationships related to the distances d_2, d_3, and d_4 in these smaller triangles were modelled using the sine theorem. Angle values for α were calculated for each model. These calculated values were evaluated considering the vehicle position.

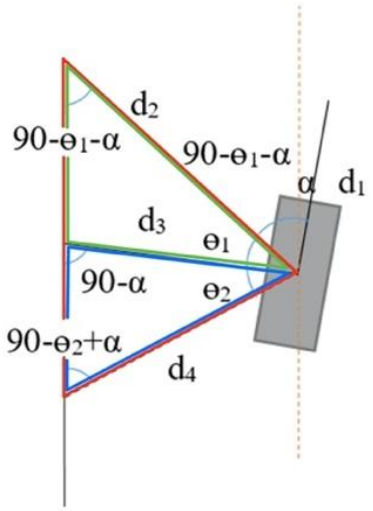

Figure 4. Formation of three triangles which can be used fort he implementation of law of sines.

Model-1

The relationship established between the distances d_2, d_4, and the angles θ_1 and θ_2 using the large triangle is shown in Equation 5. Following the calculations, the angle α is calculated as in Equation 6.

$$\frac{d_2}{\sin(90-\theta_2+\alpha)} = \frac{d_4}{\sin(90-\theta_1-\alpha)} \quad (5)$$

$$\alpha = \tan^{-1}\left[\frac{(d_2\cos\theta_1 - d_4\cos\theta_2)}{(d_4\sin\theta_2 + d_2\sin\theta_1)}\right] \quad (6)$$

Model-2

The relationship between the distances d_2, d_3, and angle θ_1, using the upper small triangle, is shown in Equation 7. According to Model 2, the angle α is calculated using Equation 8.

$$\frac{\sin(90-\theta_1-\alpha)}{d_3} = \frac{\sin(90+\alpha)}{d_2} \quad (7)$$

$$\alpha = \tan^{-1}\left(\frac{d_2\cos\theta_1 - d_3}{d_2\sin\theta_1}\right) \quad (8)$$

Model -3

The relation shown in Equation 9 was established using the lower small triangle, and by performing intermediate operations, the α angle was calculated for Model 3 using Equation 10.

$$\frac{\sin(90-\theta_2+\alpha)}{d_3} = \frac{\sin(90-\alpha)}{d_4} \quad (9)$$

$$\alpha = \tan^{-1}\left(\frac{(d_3 - d_4 \cos\theta_2)}{d_4 \sin\theta_2}\right) \quad (10)$$

4. Case Study

As part of this study, nine HC SR04 ultrasonic sensors were placed at different angles on metal plates, with three sensors per plate, and distance measurements were taken from a specific distance to the wall. Initially, the codes were developed so that each sensor would take three measurements and calculate the average of these measurements as the distance value. However, due to sensor sensitivities not being at the desired level, the codes were later modified to have each sensor take five measurements and select the smallest measurement, repeating this process three times. The average of these smallest measurements was calculated as the distance value. In this way, excessive measurements were prevented from affecting the results to a great extent and more consistent results were obtained. The sensor placement diagram is shown in Figure 5. The placement angles were set to 15˚, 20˚, and 25˚.

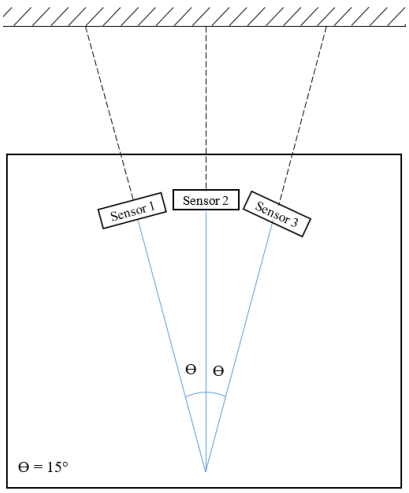

Figure 5. Representation of sensor positions for the 15 degrees alignment.

The vehicle's direction angle may deviate to the right or left for various reasons, as shown in Figure 6.

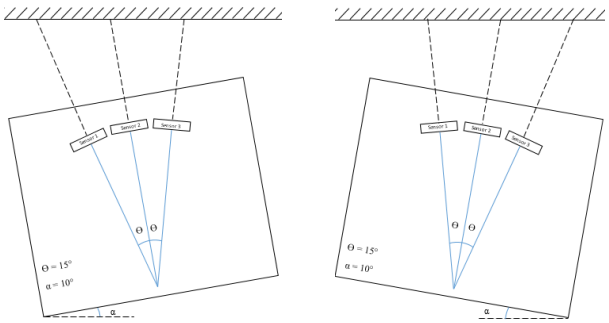

Figure 6. Illustration of sensor alignment when the heading angle deviates.

Measurements were made at different angles to determine the optimum placement angle. The placement diagrams for 20˚ and 25˚ are shown in Figures 7 and 8.

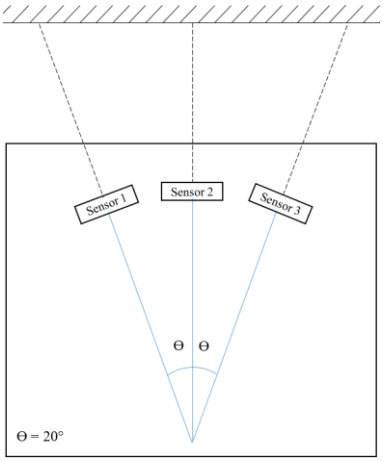

Figure 7. Representation of sensor positions for the 20 degrees alignment.

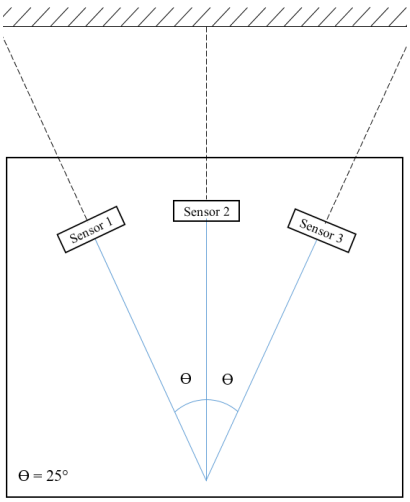

Figure 8. Representation of sensor positions for the 25 degrees alignment.

In the measurement setup, three ultrasonic sensors were mounted on metal plates at different angles, as shown in Figure 9. The plates were placed on a table to ensure vibration and positional stability and to facilitate measurement and control. A flat, homogeneous white surface was positioned opposite the sensors as a reference surface for distance measurements. As part of the study, the distances between each sensor and the reference surface were measured and recorded separately. This allowed for analysis of measurement values obtained from different situations.

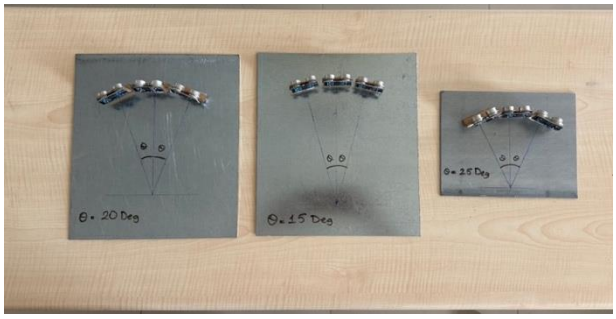

Figure 9. Illustration of the assembled sensors with 20, 15, and 25 degrees, respectively.

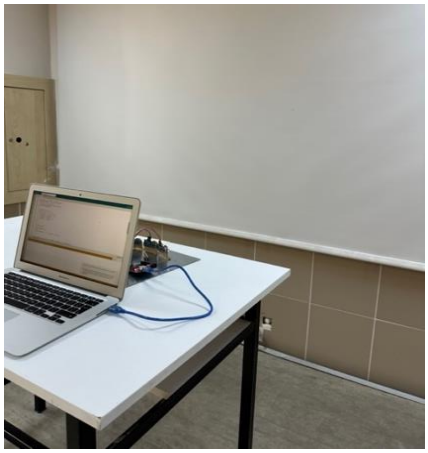

Figure 10. Test measurements done by the developed sensor constellation.

In the first stage, distance measurements were performed by positioning the sensors perpendicular to the white surface. In this case, the vehicle's deviation angle was expected to be 0 degrees. In subsequent stages, the measurements were repeated by rotating the flat plates approximately 10 degrees to the right and left, respectively. This clearly demonstrates the impact of angular changes on the measured values. Furthermore, the angular sensitivity of the sensors was analysed, and performance was compared under different orientation conditions. In the final stage, the plates were placed on the autonomous vehicle and the distance between the wall and the vehicle was measured.

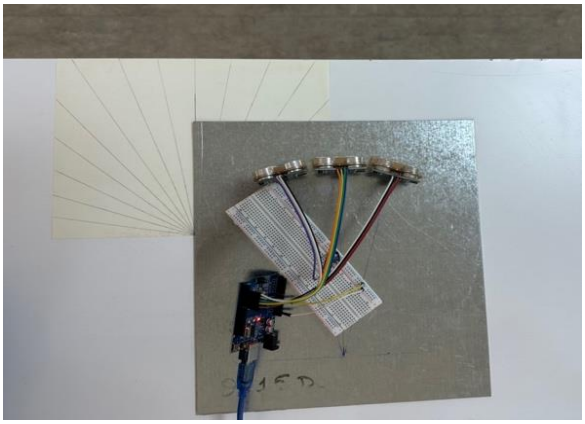

Figure 11. Measurement of deviation heading on the calibrated testing apparatus and measurement with the developed system.

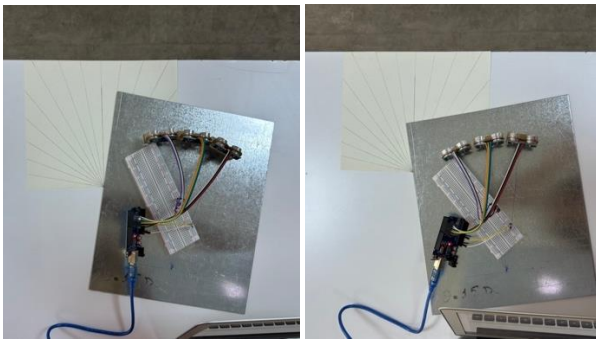

Figure 12. Testing the developed system when the heading is deviated.

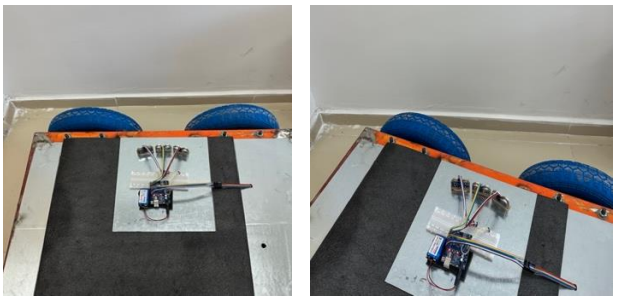

Figure 13. The developed system is tested when it is assembled on an unmanned ground vehicle.

The measurements obtained were recorded for 15 degrees when the vehicle was moving straight and deviated 10 degrees to the right and 10 degrees to the left and are given in Table 1. Similar situations were also carried out for 20 and 25 degree placements and are given in Tables 2 and 3 respectively.

$\boldsymbol{\theta} = 15^{\circ}$ $\boldsymbol{\alpha} = 0^{\circ}$					
Distance 1 (d4) (cm)	Distance 2 (d3) (cm)	Distance 3 (d2) (cm)	Model-1 $\boldsymbol{\alpha}$ (deg)	Model-2 $\boldsymbol{\alpha}$ (deg)	Model-3 $\boldsymbol{\alpha}$ (deg)
122,00	120,80	122,20	0,22	-4,87	5,32
121,40	121,30	122,10	0,63	-6,10	7,38
121,50	121,60	121,80	0,29	-7,10	7,69
121,20	121,30	122,10	0,78	-6,03	7,61
121,20	121,70	122,20	0,91	-6,60	8,45
$\boldsymbol{\theta} = 15^{\circ}$ $\boldsymbol{\alpha} = -10^{\circ}$					
126,60	123,20	122,10	-3,89	-9,58	1,67
130,30	123,50	122,10	-6,98	-10,04	-4,08
125,10	124,30	122,20	-2,50	-11,24	6,16
125,00	123,90	122,00	-2,60	-10,76	5,47
124,30	123,90	122,30	-1,70	-10,20	6,74
$\boldsymbol{\theta} = 15^{\circ}$ $\boldsymbol{\alpha} = 10^{\circ}$					
121,60	122,70	123,50	1,69	-6,13	9,57
121,00	121,70	123,20	1,90	-4,91	8,78
120,70	122,10	124,60	3,44	-3,05	10,04
120,10	121,70	124,30	3,68	-2,94	10,41
120,10	121,90	124,00	3,44	-3,67	10,67

Table 1. Test measurements conducted for the sensor constellation of 15 degrees

$\theta = 20^\circ$ $\alpha = 0^\circ$					
Distance 1 (d4) (cm)	Distance 2 (d3) (cm)	Distance 3 (d2) (cm)	Model-1 α (deg)	Model-2 α (deg)	Model-3 α (deg)
121,60	117,10	121,40	-0,11	-4,19	3,96
121,00	116,90	121,40	0,24	-3,95	4,44
121,20	117,00	122,00	0,51	-3,22	4,27
121,00	117,00	122,50	0,98	-2,49	4,49
122,20	117,10	122,20	0,01	-3,09	3,12
$\theta = 20^\circ$ $\alpha = -10^\circ$					
125,10	119,10	119,80	-3,41	-9,04	2,04
126,40	118,80	119,20	-4,59	-9,52	0,13
125,50	119,10	119,80	-3,68	-9,08	1,53
125,70	119,20	119,80	-3,77	-9,30	1,56
126,10	119,20	119,90	-3,92	-9,07	1,04
$\theta = 20^\circ$ $\alpha = 10^\circ$					
118,10	118,00	119,80	1,13	-7,50	9,83
117,10	117,80	119,50	1,58	-7,73	11,00
119,10	118,10	119,40	0,19	-8,30	8,69
119,10	118,40	119,40	0,19	-8,72	9,12
117,30	118,10	121,00	2,42	-6,16	11,17

Table 2. Test measurements conducted for the sensor constellation of 20 degrees

$\theta = 25^\circ$ $\alpha = 0^\circ$					
Distance 1 (d4) (cm)	Distance 2 (d3) (cm)	Distance 3 (d2) (cm)	Model-1 α (deg)	Model-2 α (deg)	Model-3 α (deg)
129,40	126,80	131,40	0,93	-7,87	9,83
129,50	126,80	129,80	0,10	-9,52	9,74
129,60	126,80	129,30	-0,11	-9,96	9,72
128,70	126,80	129,70	0,46	-9,56	10,54
129,50	126,80	129,30	-0,11	-10,00	9,77
$\theta = 25^\circ$ $\alpha = -10^\circ$					
127,90	124,10	124,80	-1,48	-11,71	8,60
127,60	123,80	126,20	-0,68	-10,04	8,61
212,30	125,00	125,90	-28,69	-11,57	-36,89
184,50	125,00	126,20	-21,91	-11,20	-28,45
128,10	124,10	124,50	-1,72	-12,00	8,39
$\theta = 25^\circ$ $\alpha = 10$					
114,60	113,10	115,40	0,42	-9,90	10,79
114,50	113,60	114,90	0,21	-11,03	11,56
114,50	112,90	115,10	0,32	-10,00	10,68
112,40	111,70	113,20	0,43	-10,77	11,69
115,50	113,70	115,90	0,21	-10,02	10,47

Table 3. Test measurements conducted for the sensor constellation of 25 degrees

5. Results and Discussion

This study aimed to determine the deflection of vehicle's heading angle using an algorithm based on the sine theory. This is achieved by using three ultrasonic distance sensors placed at different angles. It was observed that increasing the angle between the sensors increased the inconsistencies in the measurement results. This can be due to several factors. Ultrasonic sensors achieve the most accurate measurements when waves are sent perpendicular to the surface. As the angle increases, the sound waves scatter in different directions rather than returning directly from the surface, preventing the sensors from receiving sufficient echo signals. Furthermore, oblique reflections create a multipath effect, which can cause the signal to bounce off different surfaces and reach the sensor instead of returning directly. Furthermore, increasing the angle increases the distance the signal must travel, thus weakening the strength of the returned signal. For these reasons, measurements have also proven that increasing the angle between sensors reduces the reliability of measurements.

As a result of the measurements, Model 1, which uses the d_2 and d_4 distance values, yielded the most consistent results when the vehicle was moving parallel to the wall, meaning the deviation angle was 0 degrees. For the situation where the vehicle's heading angle deviated to the right, Model 3, which uses the d_3 and d_4 distance values, yielded the most effective results. During a right turn, the d_2 distance can have extreme values, or because the signal is reflected from a very inclined surface, multiple reflections can occur, resulting in unusable values. Since Model 3 does not require the d_2 distance for calculations, it uses the consistent d_3 and d_4 distances and produces accurate results for turning right. Similarly, Model 2 yields the most accurate results for turning left. The d_4 value in the calculations for turning left is also used.

Tests conducted under controlled and consistent measurement conditions demonstrated that the proposed method can accurately estimate the deviation angle. This finding demonstrates that the method is mathematically valid and applicable.

Ultrasonic distance sensors were preferred in the experimental studies to keep costs low. However, the structure of these sensors and their sensitivity to environmental conditions resulted in limited repeatability in measurements. Small measurement errors can lead to large errors in declination angle calculations, significantly impacting system performance. Consequently, the developed sine theory-based approach can produce accurate and stable results when reliable distance data is provided.

References

Boschert, S., Heinrich, C., & Rosen, R. (2018, May). Next generation digital twin. In Proc. tmce (Vol. 2018, pp. 7-11). Las Palmas de Gran Canaria, Spain.

El Jazzar, M., Piskernik, M., & Nassereddine, H. (2020, July). Digital twin in construction: An empirical analysis. In EG-ICE 2020 Workshop on Intelligent Computing in Engineering, Proceedings (pp. 501-510).

Grieves, M. (2014). Digital twin: manufacturing excellence through virtual factory replication. White paper, 1(2014), 1-7.

Hasan, S. M., Lee, K., Moon, D., Kwon, S., Jinwoo, S., & Lee, S. (2022). Augmented reality and digital twin system for interaction with construction machinery. Journal of Asian Architecture and Building Engineering, 21(2), 564-574.

Khaleel, H. Z., & Oleiwi, B. K. (2024). Ultrasonic sensor decision-making algorithm for mobile robot motion in maze environment. Bulletin of Electrical Engineering and Informatics, 13(1), 109-116.

Negri, E., Fumagalli, L., & Macchi, M. (2017). A review of the roles of digital twin in CPS-based production systems. Procedia manufacturing, 11, 939-948.

Pandian, J. A., Karthick, R., & Karthikeyan, B. (2012). Maze solving robot using freeduino and LSRB algorithm. International Journal of Modern Engineering Research, 56, 92-100.

Qi, Q., & Tao, F. (2018). Digital twin and big data towards smart manufacturing and industry 4.0: 360 degree comparison. *Ieee Access*, *6*, 3585-3593.

Shafto, M., Conroy, M., Doyle, R., Glaessgen, E., Kemp, C., LeMoigne, J., & Wang, L. (2010). Draft modeling, simulation, information technology & processing roadmap. Technology area, 11, 1-32.

Suryanarayana, S., & Akhila, V. (2021). Autonomous maze solving robot using arduino. Technology (IJARET), 12(3), 595-603.

Suthar, S., & Shukla, V. (2023, December). Intelligent Non-Looped Maze Solving Robot: IR Sensor-Driven Autonomous Navigation. In 2023 IEEE Technology & Engineering Management Conference-Asia Pacific (TEMSCON-ASPAC) (pp. 1-5). IEEE.

Yoo, Y., Lyytinen, K. J., Boland, R. J., & Berente, N. (2010). The next wave of digital innovation: Opportunities and challenges: A report on the research workshop'Digital Challenges in Innovation Research'.

Zhuang, C., Miao, T., Liu, J., & Xiong, H. (2021). The connotation of digital twin, and the construction and application method of shop-floor digital twin. Robotics and Computer-Integrated Manufacturing, 68, 102075.